energies

Article

Evaluation Method of the Incremental Power Supply Capability Brought by Distributed Generation

Yi Hao [1], Zhigang Huang [1], Shiqian Ma [2], Jiakai Huang [2], Jiahao Chen [3] and Bing Sun [3,*]

[1] State Grid Tianjin Electric Power Company, Tianjin 300010, China
[2] State Grid Tianjin Electric Power Research Institute, Tianjin 300010, China
[3] School of Electrical Automation and Information Engineering, Tianjin University, Tianjin 300072, China
* Correspondence: sunbing@tju.edu.cn

Abstract: More and more distributed generation (DG) and energy storage (ES) devices are being connected to the distribution network (DN). They have the potential of maintaining a stable supply load during failure periods when using islanding operations. Therefore, DG and ES have capacity value, i.e., improving the power supply capability of the system. However, there are strong fluctuations in DG outputs, and the operations of ES devices have sequential characteristics. The same capacity of DG has different load-bearing capabilities compared to conventional thermal or hydroelectric units. This paper proposes a method for evaluation of power supply capability improvement in DNs. First, the temporal fluctuation in both power source and load demand during fault periods is considered. A DN island partition model considering the secondary power outage constraint is established. Then, a modified genetic algorithm is designed. The complex island partition model is solved to achieve accurate power supply reliability evaluation. And the incremental power supply capability associated to DG and ES devices is calculated. Finally, a case study is conducted on the PG&E 69-bus system to verify the effectiveness of the proposed method. It is found that with a 20% configuration ratio of ES devices, the power supply capability improvement brought about by 6 MW DG can reach about 773 kW.

Keywords: power supply capability; distributed generation; power supply reliability criteria; island partition; genetic algorithm

Citation: Hao, Y.; Huang, Z.; Ma, S.; Huang, J.; Chen, J.; Sun, B. Evaluation Method of the Incremental Power Supply Capability Brought by Distributed Generation. *Energies* **2023**, *16*, 6062. https://doi.org/10.3390/en16166062

Academic Editors: Vivek Prakash, Bhanu Pratap Soni and Kailash Chand Sharma

Received: 23 July 2023
Revised: 16 August 2023
Accepted: 17 August 2023
Published: 18 August 2023

1. Introduction

To realize the grand goal of "double carbon", China has been vigorously developing wind power generation, photovoltaic (PV) energy generation, and other renewable energy sources, of which distributed generation (DG) is an important part [1]. However, the active power of wind turbines and PV units is volatile, and their gradual integration will pose challenges to the normal operation of the power system. Therefore, the National Development and Reform Commission and other departments have issued relevant documents requiring that some ES devices must be configured, when investing in renewable energy in the future, to suppress fluctuations in renewable power output [2]. The integration of DG and ES devices into various levels of the DN in the load center can help to achieve on-site development and consumption of electricity, save construction and maintenance costs associated with the power grid, increase the power supply capability of the distribution system, and reduce network losses [3]. The capacity value of DG devices plays an important role in maintaining reliable DN operations. During system failures, they can continue to supply locally important loads through "islanding" operations, thus improving power supply reliability [4].

Therefore, the integration of various DG devices can reduce the dependence of the DN on the higher-level power grid and improve the power supply capability of the DN. The installed capacity of DG and ES devices cannot represent the incremental power supply capability. If a certain proportional coefficient is set—such as 10% of the installed capacity—it may lack credibility. There are various methods that can be used for evaluation of the power supply capability. Early power supply capability evaluation methods often considered the rated capability of substations separately, using the substation capacity-to-load ratio index [5] for measurements. In addition, some scholars have proposed the concept of maximum power supply capability, which is the maximum load demand that a power system can supply, and they calculated the power supply capability index based on the repetitive power flow method [6]. However, this method does not solve the problem of the system capacity range under different load distributions. There are also studies that have suggested measuring power supply capability through the safe boundary power supply capability, but this approach does not take the uncertainty of renewable energy output into consideration [7]. In the specific scenario of evaluating the power supply capability of DNs with DG devices, conducting a capacity-value evaluation of the DG devices [8] and quantifying this capacity value provides an effective way to measure the power supply capability [9]. Researchers have attempted to find alternative scientific methods to more accurately determine the power supply capability [10]. However, according to relevant IEEE standards, the power supply capability cannot be described independently. The power supply capability should be mentioned only along with a clear description of the power supply reliability. In 1966, L. Garver first proposed the concept of credible capacity, based on the effective load carrying capacity [11]. Since then, credible capacity has become an important indicator for measuring the capacity of renewable power generators.

There is currently no consensus on the methods to be used for evaluation of credible capacity, which can be divided into two kinds based on whether equal reliability criteria are followed. The load curve method is a common method for evaluating the credible capacity that is not based on equal reliability. In [12], the authors compared the load duration curves of renewable energy units before and after their connection and took the load decrease as the credible capacity of renewable energy units, quickly providing a credible capacity indicator from a macro perspective. The Garver approximation method was proposed in [13], which models the wind turbine as several discrete output values and derives the credible capacity of the wind turbine. In [14], the Z-statistics method was proposed, which assumes that the redundant capacity of the system obeys a normal distribution with the fluctuation of renewable energy units and loads, and an approximate calculation formula of the credible capacity was derived. In [15], the reliability function method was proposed, which first established a power supply reliability function taking the load demand value as the key variable, and an expression for wind power credible capacity was obtained. This method is suitable for situations where the renewable energy is relatively low. In [16], neural networks were trained with empirical samples in order to calculate the credible capacity directly. However, the abovementioned methods generally require strong assumptions.

In evaluation methods based on equal reliability criteria, the selection of reliability indicators is an important part of the reliability calculation. When conducting a credible capacity search based on reliability indicators, most studies select the expected energy not served (EENS) of the power supply as the comparison standard for power supply reliability [17]. Other studies have used indicators such as the loss-of-load frequency [18], well-being framework [19], loss-of-load-expectation standard [20], and Value at Risk. To complete the power supply improvement search, existing one-dimensional search methods such as the dichotomy method [21] and the truncation method [22] can meet the computational accuracy requirements.

Fault consequence analysis is the core link in DN reliability assessments. During system failures, the DG power supply capability and the DN topology flexibility can support the recovery of important loads (i.e., through island partitioning). In the IEEE 1547.4-2011 standard [23], it is encouraged that conscious island operations should be considered, stating that planning for the island should take into account the action strategy of switches [24].

Existing methods for solving island partition models can be divided into graph theory-based methods, intelligent algorithms, and heuristic algorithms. The graph theory-based methods typically utilize an undirected graph model and transform the complex island partition model into a minimum spanning tree problem [25]. A micro-phasor measurement unit could monitor the DN in real time, so as to avoid issues related to grid stability [26]. However, current graph theoretic partition methods often have difficulty in achieving both good computational speed and accuracy. Intelligent algorithms, represented by genetic algorithms [27], differential evolution algorithms [28], and particle swarm optimization algorithms [29], possess strong universality and can solve non-linear island partition models through iterative calculations. Heuristic algorithms [30] and ordinary intelligent algorithms are both important methods for solving island partition models. However, when considering ES devices, their sequential characteristics significantly increase the complexity of solving the island partition problem, and there is relatively little research on island partitioning that takes into account ES operations.

In summary, in order to evaluate the improvement effect of DG devices on the power supply capability of DNs, it is necessary to evaluate the united credible capacity of DG and ES. Existing research still has the following shortcomings: (1) the fault consequence analysis does not consider the island partition, or the island partition model ignores the flexible change in the DN topology, and most of them do not consider secondary power outage constraints; and (2) it only considers the capacity value of DG devices, without considering the ability to suppress the DG output after the integration of ES devices. As such, effective scheduling methods for ES devices during failures are lacking.

In response to the shortcomings in the existing literature, this paper proposes a method for evaluation of the improved effectiveness of the power supply capability in a DN based on credible capacity. First, combined with the calculation principles of credible capacity, the concept of incremental power supply capability brought by DG and ES devices is expressed. Second, in order to take advantage of the diversification of electricity sources and flexibility of the topological structure of distribution networks, an island partition model is established to estimate the power supply reliability of the distribution network. Finally, to account for the secondary power outage constraint and island network topology connectivity constraint, a genetic algorithm solution strategy is proposed, thus realizing fast computation. The logical framework of this paper is shown in the following Figure 1.

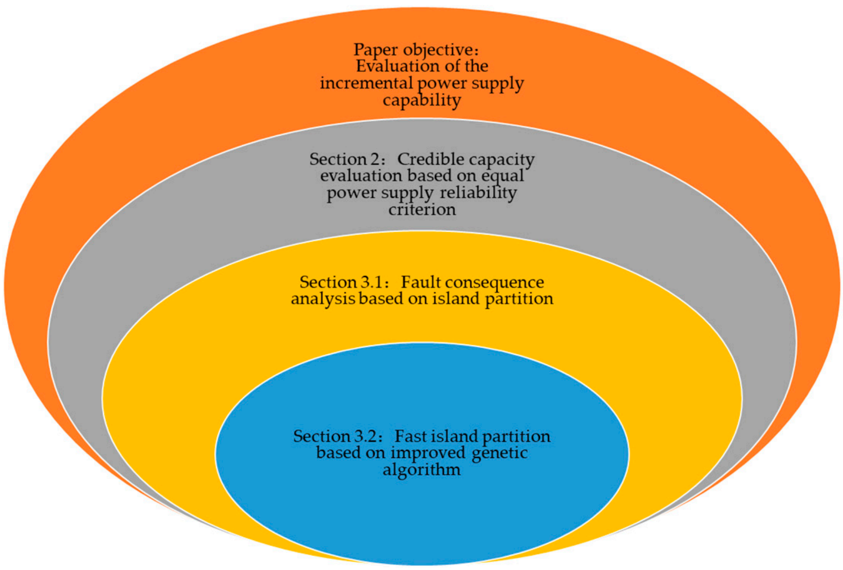

Figure 1. The logical relationships between the sections in this paper.

2. The Method for Calculating Increased Power Supply Capability

The traditional distribution network obtains electrical energy from the upper power grid and uses feeders to distribute electrical energy to each load node. If a feeder fails, resulting in power outages for some users, the power supply to important loads can be restored in time through measures such as switching operations. Assuming that the available upper grid power supply capability of the DN is C_{con} and the load level is L_0, the power supply reliability level can be denoted as $Re\{C_{\mathrm{con}}, L_0\}$. L_0 denotes the original load demand and is represented by the annual maximum active power. According to the theory of power supply reliability, an increase in the number of generators can improve power supply reliability, while an increase in the load demand can downgrade reliability. For quantification of the value of $Re\{C_{\mathrm{con}}, L_0\}$, there are four basic steps: component modeling, system operation state generation, failure consequence analysis, and reliability index calculation (for the detailed process, we refer the reader to [31]).

The integration of distributed renewable energy sources and energy storage batteries promotes the diversification of energy sources in smart distribution networks. Therefore, after the integration of renewable energy units and ES devices—whose capacities are denoted as C_{ren} and C_{ES}, respectively—into the DN, the power supply reliability is improved as $Re\{C_{\mathrm{con}} + C_{\mathrm{ren}} + C_{\mathrm{ES}}, L_0\}$ from $Re\{C_{\mathrm{con}}, L_0\}$. If the load level increases to $L_0 + \Delta L$, the power supply reliability level of the DN recovers to $Re\ \{C_{\mathrm{con}}, L_0\}$. Then, the increase in load supply capacity ΔL is called the credible capacity of DG and ES. Credible capacity assessment is a one-dimensional search process that requires repeated calculations to determine the level of load improvement that meets the equivalent power supply reliability criteria. A binary method can be used to effectively implement the one-dimensional search process. The specific steps of searching for the credible capacity are as follows:

(1) Calculate the EENS index caused by system failures and evaluate the current reliability level $Re\{C_{\mathrm{con}}, L_0\}$.
(2) Integrate DG and ES devices with respective capacities C_{ren} and C_{ES} into the network, while keeping the system load level L_0 unchanged. The improved power supply reliability is denoted as $Re\{C_{\mathrm{con}} + C_{\mathrm{ren}} + C_{\mathrm{ES}}, L_0\}$. The initial value l_1 is set to 1.
(3) Raise the load demand to $L_0 + l_1 \times L'$; update the power supply reliability, which is denoted as $Re\{C_{\mathrm{con}} + C_{\mathrm{ren}} + C_{\mathrm{ES}}, L_0 + l_1 \times L'\}$; and determine whether $Re\{C_{\mathrm{con}} + C_{\mathrm{ren}} + C_{\mathrm{ES}}, L_0 + l_1 \times L'\}$ is greater than $Re\{C_{\mathrm{con}}, L_0\}$. L' denotes the searching step used while seeking the incremental power supply capability, and l_1 denotes the accounting number of searching steps. If yes, proceed to step (5); otherwise, proceed to step (4).
(4) Let $l_1 = l_1 + 1$; return to step (3).
(5) The incremental load demand corresponding to the credible capacity is between $[L_0 + (l_1 - 1) \times L', L_0 + l_1 \times L']$. At this point, the obtained $\Delta L = l_1 \times L'$ is the DG credible capacity. The schematic diagram of completing one credible capacity search is depicted in Figure 2.

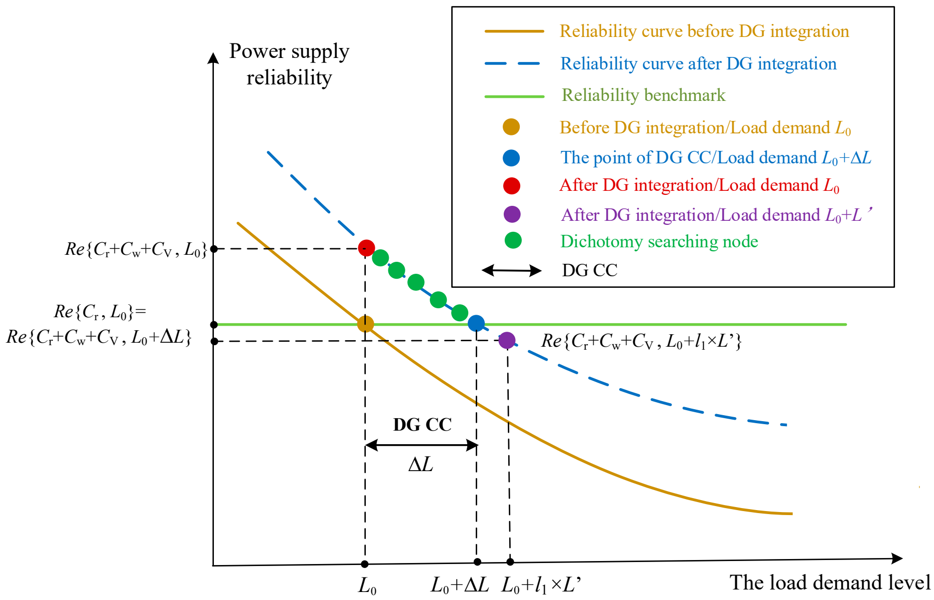

Figure 2. The schematic diagram of incremental power supply capability search.

3. Power Supply Reliability Evaluation Method Based on Island Partition

According to the theory detailed above, it is necessary to evaluate the power supply reliability value, during which the influence of DG and ES devices must be accounted for accurately.

3.1. Island Partition Model

The core of evaluating the credible capacity of DG and ES devices is searching for an accurate load improvement level ΔL. This paper takes the EENS as the system reliability indicator, and the sequential Monte Carlo method is used for power supply reliability evaluation. When evaluating the power supply reliability of the DN, it is necessary to conduct fault consequence analysis based on the island partition.

After a system failure, if DG and ES devices are not considered, the total power outage during the failure period is E_{total}. The remaining EENS index after adopting island partition measures is recorded as E_{NS}, and its calculation method is shown in Equation (1):

$$E_{\text{NS}} = E_{\text{total}} - \sum_{t=1}^{T} \sum_{a=1}^{A} \sum_{i\in\mathbf{\Omega}_a} P_{i,t}^{\text{load}}, \tag{1}$$

where $P_{i,t}$ represents the active output of node i at time t, T represents the duration of the fault, N represents the set of nodes, A represents the number of islands, and $\mathbf{\Omega}_a$ represents the set of nodes within the a_{th} island.

The purpose of island partitioning is to restore power supply to more important loads in the DN. The objective function is used to minimize the potential power outage loss of load nodes within the island, as shown in Equation (2):

$$\min \sum_{i\in N} [(1 - ST_i) \times \sum_{t=t_1}^{t_2} B_{i,t}], \tag{2}$$

where $B_{i,t}$ represents the reduced power outage loss of node i due to power restoration at time t, t_1 represents the beginning time of the fault, and t_2 represents the end time of the fault. ST_i and $st_{i,t}$ represent whether node i is included in the island. These are both 0–1 binary variables: if node i is put in the island at time t, then $st_{i,t}$ is 1; otherwise, it is 0. This model comprehensively considers many factors such as the source load fluctuation, load priority, and secondary power outage constraints, as well as the flexible operation and radial structure constraints of connecting lines in the DN.

$$\left\{\begin{array}{l}
ST_i = \left\{\begin{array}{l} 1\ if\ st_{i,t} = 1 \ \ \forall i \in \boldsymbol{N}, \forall t \in [t_1, t_2] \\ 0\ if\ st_{i,t} = 0 \ \ \forall i \in \boldsymbol{N}, \forall t \in [t_1, t_2] \end{array}\right. \\
st_{i,t} = \left\{\begin{array}{l} 1 \ \ if\ i \in \bigcup\limits_{a=1}^{A} \boldsymbol{\Omega}_a \ \ \forall i \in \boldsymbol{N},\ \forall t \in [t_1, t_2] \\ 0 \ \ if\ i \notin \bigcup\limits_{a=1}^{A} \boldsymbol{\Omega}_a \ \ \forall i \in \boldsymbol{N},\ \forall t \in [t_1, t_2] \end{array}\right. \\
B_{i,t} = P_{i,t}^{\text{load}} * PR_i \ \ \ \forall i \in \boldsymbol{N},\ \forall t \in [t_1, t_2] \\
\beta_{ij} + \beta_{ji} = \omega_{ij} \ \ \ \forall i \in \boldsymbol{\Omega}_a, j \in \boldsymbol{NB_i}, \forall a \in [1, A] \\
\beta_{ij} = 0 \qquad \forall i \in \boldsymbol{\Lambda}_a, \forall a \in [1, A] \\
\beta_{ij} \in \{0,\ 1\} \qquad \forall i \in \boldsymbol{\Omega}_a / \boldsymbol{\Lambda}_a, j \in \boldsymbol{NB_i}, \forall a \in [1, A] \\
\sum\limits_{j \in \boldsymbol{NB}_i} \beta_{ij} = 1 \ \ \ \forall i \in \boldsymbol{\Omega}_a, \forall i \notin \boldsymbol{\Lambda}_a, \forall a \in [1, A] \\
0 \leq \omega_{ij} \leq 1 \ \ \ \forall i \in \boldsymbol{\Omega}_a, j \in \boldsymbol{NB}_i, \forall a \in [1, A] \\
\boldsymbol{\Omega}_a \cap \boldsymbol{\Omega}_b = \varnothing \ \ \ \forall a \in [1, A],\ b \in [1, A],\ a \neq b \\
\boldsymbol{\Lambda}_a \cap \boldsymbol{\Lambda}_b = \varnothing \ \ \ \forall a \in [1, A],\ b \in [1, A],\ a \neq b \\
PG_{i,t} \leq PG_{i,t}^{\max} \ \ \ \forall i \in \boldsymbol{\Lambda}_a, \forall a \in [1, A],\ \forall t \in [t_1, t_2] \\
\sum\limits_{i \in \boldsymbol{\Omega}_a} P_{i,t}^{\text{load}} * st_{i,t} = \sum\limits_{j \in \boldsymbol{\Lambda}_a} P_{j,t}^{\text{dis}} - P_{j,t}^{\text{cha}} + PG_{j,t} \ \ \forall a \in [1, A],\ \ \forall t \in [t_1, t_2] \\
E_{\min} \leqslant E_{i,t} \leqslant E_{\max} \ \ \forall i \in \boldsymbol{\Lambda}_a, \forall t \in [t_1, t_2] \\
E_{i,t_1} = E_0 \ \ \forall i \in \boldsymbol{\Lambda}_a \\
E_{i,t} = E_{i,t-1} - P_{i,t}^{\text{dis}} + P_{i,t}^{\text{cha}} \ \ \forall i \in \boldsymbol{\Lambda}_a, \forall t \in [t_1, t_2] \\
0 \leq u_{i,t}^{\text{cha}} + u_{i,t}^{\text{dis}} \leq 1 \ \ \forall i \in \boldsymbol{\Lambda}_a, \forall t \in [t_1, t_2] \\
E_{\max} * u_{i,t}^{\text{cha}} * \beta_{\min} \leq P_{i,t}^{\text{cha}} \leq E_{\max} * u_{i,t}^{\text{cha}} * \beta_{\max} \ \ \forall i \in \boldsymbol{\Lambda}_a, \forall t \in [t_1, t_2] \\
E_{\max} * u_{i,t}^{\text{dis}} * \beta_{\min} \leq P_{i,t}^{\text{dis}} \leq E_{\max} * u_{i,t}^{\text{dis}} * \beta_{\max} \ \ \forall i \in \boldsymbol{\Lambda}_a, \forall t \in [t_1, t_2]
\end{array}\right. \tag{3}$$

If all the values of $st_{i,t}$ for node i during the fault period $[t_1, t_2]$ are 1, then $ST_i = 1$; otherwise, it is equal to 0. Therefore, the island scheme decision variable ST_i is achieved by taking the intersection of the $st_{i,t}$ values during the fault period $[t_1, t_2]$. The island benefit $B_{i,t}$ is composed of the product of the active power $P_{i,t}$ of the load within the island and the priority weight PR_i. β_{ij} and β_{ji} are both 0–1 variables representing whether the DN maintains radial operations. ω_{ij} is a 0–1 variable representing whether a switch is open or closed. $\boldsymbol{\Lambda}_a$ represents the set of load points with DG and ES devices connected within the a^{th} island. $\boldsymbol{NB}_i$ represents adjacent nodes of node i. The DG output is denoted as $PG_{i,t}$, and t cannot exceed its predicted output upper limit $PG_{i,t}^{\max}$. $P_{j,t}^{\text{cha}}$ and $P_{j,t}^{\text{dis}}$ represent the ES charging and discharging capacities connected to node j at time t, respectively. $E_{i,t}$ represents the remaining ES at time t at node i, while $E_{\min}$ and $E_{\max}$ are the lower and upper limits of the state of charge. $u_{i,t}^{\text{cha}}$ is a 0–1 variable representing whether the ES device is in charging state, with 1 denoting charging. $u_{i,t}^{\text{dis}}$ is a 0–1 variable representing whether the ES is in discharging state, with 1 denoting discharging. $\beta_{\min}$ and $\beta_{\max}$ are the upper and lower limit parameters, respectively, for ES charging and discharging.

The first two formulas of Equation (3) represent the secondary power outage constraint, and the nodes drawn into the island cannot experience a secondary power outage under the fault state. The third formula of Equation (3) represents the island benefit calculation method, which is taken as the objective function of the island partition model. The 4th to 8th formulas of Equation (3) represents the radial operation constraints of the DN, which ensure that there is no ring network within the island. The 9th to 10th formulas of Equation (3) represents the island non-joint constraint, which means that each DG device and load node can only operate on a portion of one island (i.e., they cannot belong to two islands at the same time). The eleventh formula of Equation (3) represents the upper limit constraint of the DG output. The twelfth formula of Equation (3) represents the power and electricity balance constraint. The 13th to 18th formulas of Equation (3) represents the relevant operational constraints of ES devices.

The optimization variable of the island model is whether each node is drawn into the island, denoted by the variable ST_i. If the ST_i value of node i is 1, it indicates that node i is restored; meanwhile, if its value is 0, node i is not restored. The optimization objective of the island partition model is the weighted benefit of the total restored load $B_{i,t}$. It should be emphasized that non-linear node voltage limits and branch power flow constraints are not considered in Equation (3). For the island partition scheme developed using the above model, it is necessary to check whether the node voltage and branch power flow requirements are met. If the node voltage or the branch current exceeds the limit, it is necessary to cut off leaf load nodes of the islands to meet the voltage and thermal constraints. As this is not the core work of this paper, further details along these lines are not provided.

3.2. A Method for Quickly Solving the Island Partition Model

The island partition results are closely related to the remaining electricity at the fault beginning time, and, so, a reasonable calculation method for the remaining ES must be established.

3.2.1. Calculation Method for Remaining Electricity at Fault Beginning Time

In developing island partition schemes, the remaining electricity in the ES devices at the beginning time of a failure is a critical parameter. As the sequential Monte Carlo method is used for evaluation of the reliability, it is convenient to simulate the continuous change in the running state of the system. The ES devices in the DN can perform various functions, and the main scheduling goal during normal operations of the DN is to cut the peaks and fill the valleys, where peak and valley electricity prices are used to arbitrage and promote the efficient consumption of renewable energy. The purchase cost and sales revenue of the DN are recorded as C_1, the network loss cost of the DN is recorded as C_2, and the ES loss cost is recorded as C_3. Therefore, the system operation cost can be calculated as follows:

$$C = C_1 + C_2 + C_3 = \sum_{t=1}^{T} (C_{t,\text{buy}} P_{t,\text{buy}}^{\text{tra}} - C_{t,\text{sell}} P_{t,\text{sell}}^{\text{tra}}) + C_t \sum_{t=1}^{T} \sum_{ij \in \boldsymbol{B}} I_{ij,t}^2 R_{ij} + C_{\text{ES}} \sum_{t=1}^{T} \sum_{i=1}^{N_{\text{ES}}} \max\left\{ P_{i,t}^{\text{dis}}, P_{i,t}^{\text{cha}} \right\}, \tag{4}$$

where $C_{t,\text{buy}}$ and $C_{t,\text{sell}}$ represent the unit prices for purchasing and selling electricity between the DN and the superior grid at time t, respectively; $P_{t,\text{buy}}^{\text{tra}}$ and $P_{t,\text{sell}}^{\text{tra}}$ represent the power of purchasing and selling electricity from the superior power grid at time t, respectively; C_t represents the cost of unit network loss; $\boldsymbol{B}$ represents the collection of all branches in the DN; R_{ij} and $I_{ij,t}$ represent the branch resistance with node i as the starting point and node j as the ending point and the branch current at time t, respectively; C_{ES} represents the ES cost for 1 kWh charging/discharging; and N_{ES} represents the number of nodes with ES.

The injected power of a node should meet the power balance constraint, and the following constraint conditions were established based on the DistFlow power flow model:

$$P_{ji,t} - R_{ij} I_{ij,t}^2 - \sum_{k \in \boldsymbol{H}(i)} P_{ik,t} = P_{i,t}^{\text{load}} - P_{i,t}^{\text{PV}} - P_{i,t}^{\text{ES}}, \tag{5}$$

$$Q_{i,t}^{\text{load}} = Q_{ji,t} - x_{ij} I_{ij,t}^2 - \sum_{k \in \boldsymbol{H}(i)} Q_{ik,t}, \tag{6}$$

where $P_{ji,t}$ and $Q_{ji,t}$ represent the active and reactive power of the branch at time t flowing from node j to node i, respectively; x_{ij} represents the branch reactance between nodes i and j; $\boldsymbol{H}(i)$ represents the set of branches associated with node i; and $Q_{i,t}^{\text{load}}$ represents the reactive load of the user at node i at time t. The voltage between adjacent nodes meets the following voltage drop constraints:

$$U_{j,t}^2 = U_{i,t}^2 - 2\left(r_{ij}P_{ij,t} + x_{ij}Q_{ij,t}\right) + \left(r_{ij}^2 + x_{ij}^2\right)I_{ij,t}^2, \tag{7}$$

$$I_{ij,t}^2 = \frac{P_{ij,t}^2 + Q_{ij,t}^2}{U_{i,t}^2}, \tag{8}$$

where $U_{i,t}$ and $U_{j,t}$ represent the voltage at the beginning and end nodes of the branch with node i as the first segment and node j as the end, respectively. To make the DN operate securely, branch current and node voltage constraints are established:

$$I_{ij,t}^2 \le I_{ij,\max}^2, \tag{9}$$

$$U_{i,\min} \le U_{i,t} \le U_{i,\max}, \tag{10}$$

where $U_{i,\min}$ and $U_{i,\max}$ represent the lower and upper voltage limits of node i, respectively, and $I_{ij,\max}$ represents the upper branch flow current limit. The ES charging and discharging processes are detailed in Equation (3). The above day-ahead DN economic dispatch model can be solved using common second-order cone planning using commercial software, which will not be expanded on here.

3.2.2. Solving Process with Genetic Algorithm

The island partition decision variable is the ST_i value of each node. Due to the existence of radial constraints and the inability to recover load nodes at intervals, if ST_i is randomly generated for each node, it is likely that the solution will be infeasible. The island partition model is a special knapsack problem that considers radial constraints, secondary power outage constraints, power supply continuity constraints, and sequential operation constraints of ES devices. The ordinary genetic algorithm cannot solve this kind of problem directly.

This paper improves the genetic algorithm by (1) starting from the DG nodes and sequentially searching the island partition scheme for each island, and (2) for the a_{th} island scheme to be developed, the number of load nodes N_{node} gradually increases from 0, and the genetic information is a random set of nodes containing DG nodes without node jumps. At this time, the length of the gene is N_{node}.

When searching for the isolated island scheme $\boldsymbol{\Omega}_a$, the specific calculation process is as follows:

(1) Initialization: Set the number of evolutionary iterations t to a value of 0. Set the maximum number of evolutionary iterations $T_{\max}$ and randomly generate M genes with a length of N_{node} based on the node connection matrix of the DN, $\boldsymbol{GE}_m^{N_{\text{node}}}$. Each element represents the number of nodes included in $\boldsymbol{\Omega}_a$:

$$\boldsymbol{GE}_m^{N_{\text{node}}} = \left[NO_1, NO_2, \cdots, NO_{N_{\text{node}}}\right] \; m \in [1, M]. \tag{11}$$

(2) Individual fitness evaluation: Check whether the constraint conditions of Equation (3) are met, where the state of charge of the stored energy is determined according to the following logic. When the DG output is greater than the sum of the loads of all nodes, the remaining electricity will charge the ES under the condition that the ES capacity and power do not exceed the limit; otherwise, the DG and ES will both supply power to the load, and the state in which the ES capacity is less than the minimum value of the state of charge will occur, which means that the constraint conditions are out of bounds. The fitness function of $\boldsymbol{GE}_m^{N_{\text{node}}}$ is recorded as $FI_m^{N_{\text{node}}}$. If any constraint

condition from Equation (3) is out of its limits, then $FI_m^{N_{\text{node}}} = 0$; otherwise, $FI_m^{N_{\text{node}}}$ is calculated according to the objective function in Equation (3).

(3) Selection operation: Select the individual with the best fitness and save the gene. With the help of the selection measure, the optimal individuals can be directly inherited to the next generation, and they will help to generate new individuals through the cross-mutation process.

(4) Cross operation: Randomly exchange genes from different populations with the genes of the optimal individual, ensuring population variability through cross operation on the optimal individual. The crossover process is the key step in genetic algorithms.

(5) Mutation operation: Each individual is set to change part of their individual gene values with a certain mutation rate, ensuring the richness and diversity of genes in the population.

(6) Let $t = t + 1$ and return to step (3) until $t = T_{\max}$. The best fitness function when the gene length is N_{node} is recorded as $FI_{\max}^{N_{\text{node}}}$. Next, proceed to step (7).

(7) Let $N_{\text{node}} = N_{\text{node}} + 1$; return to step (1) and re-calculate $FI_{\max}^{N_{\text{node}}}$ until the $FI_{\max}^{N_{\text{node}}}$ of the N_{node} generation is zero. The $\boldsymbol{GE}_m^{N_{\text{node}}}$ corresponding to the maximum value of all $FI_{\max}^{N_{\text{node}}}$ is the island scheme is to be solved.

For the a_{th} island that has already completed the island search, consider it equivalent to a new node and replace all nodes in $\boldsymbol{\Omega}_a$. Update the node connection matrix of the DN; then, search for the $(a + 1)_{\text{th}}$ island until all DG devices in the DN are traversed.

4. Case Study

4.1. System Parameter

Based on the method proposed in the paper, we evaluated the incremental power supply capability of the PG&E 69-node system. The topological structure of the PG&E 69-node system is shown in Figure 3, with the superior power grid regarded as an infinite power source. In particular, 1 MW PV units were connected at nodes 5 and 36, 2 MW wind turbines were connected at nodes 18 and 52, and 20% ES devices were installed at each DG node. The components considered in the DN reliability estimation included the busbars, circuit breakers, distribution transformers, and distribution feeders. The above components were modeled as operation–failure two-state models. The failure rate was 0.2 times per year, and the repair rate was set as 1000 times per year. Interconnection switches were included, as shown in Figure 3, which are considered to be open during normal system operations. The fluctuation of load demand is shown in Figure 4, and the one-year output curves for the PV equipment and wind turbine are given in Figures 5 and 6, respectively. The load priority of the PG&E 69-bus system is detailed in Table 1.

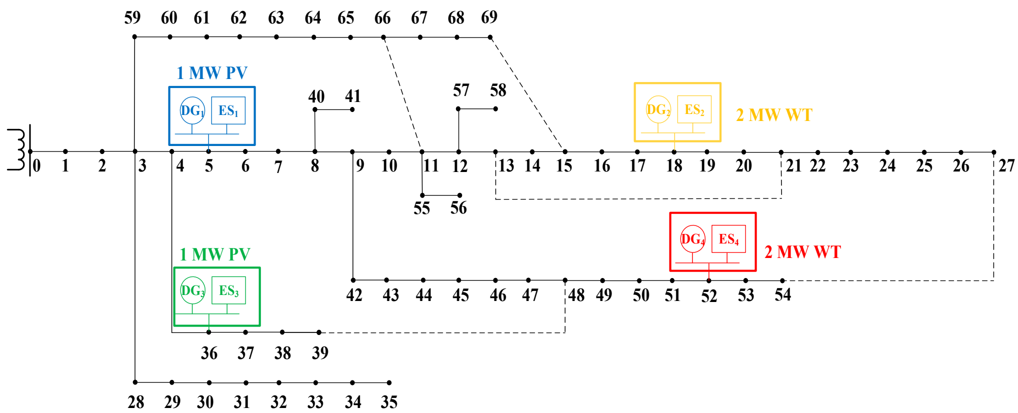

Figure 3. Topology of the PG&E 69-bus system.

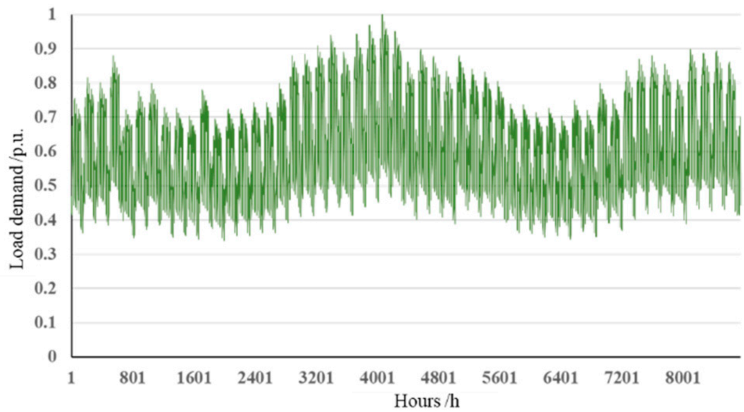

Figure 4. Fluctuation curve of load demand.

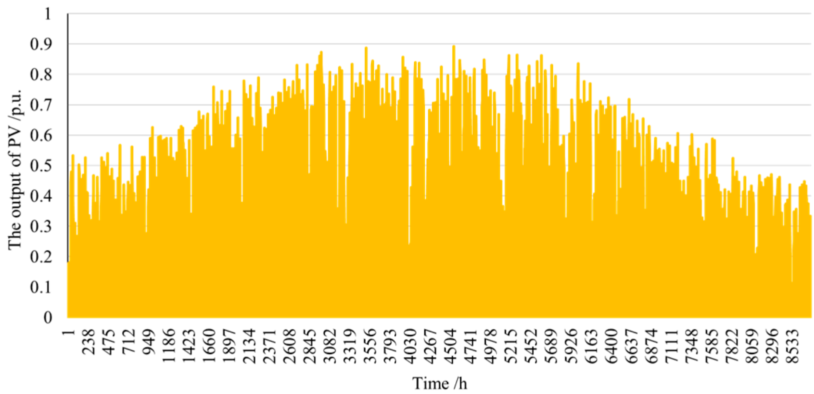

Figure 5. Output curve of PV equipment.

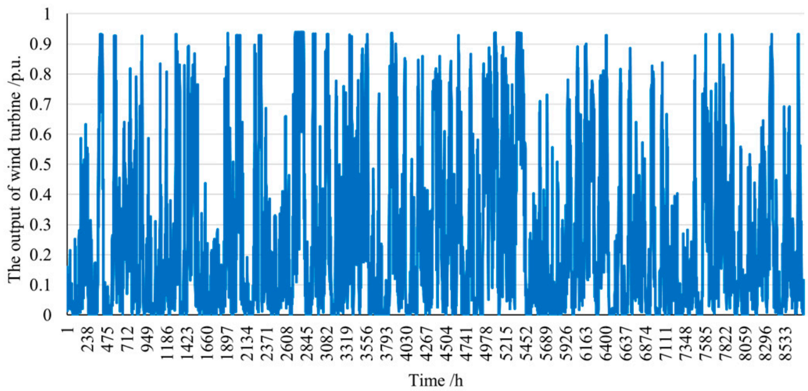

Figure 6. Output curve of wind turbine.

Table 1. Load priority of the PG&E 69-bus system.

Load Level	Priority	Load Nodes (Number)
I	100	3 4 5 6 13 14 17 18 19 27 28 29 36 37 39 51 52 54 59 66 69
II	10	1 2 7 8 9 10 11 12 15 16 20 21 22 23 26 30 31 32 38 40 42 43 44 45 46 47 48 49 50 53 55 57 63 64 65 67 68
III	1	24 25 33 34 35 41 56 58 60 61 62

4.2. Island Partition Scheme

During the reliability assessment process, based on the sequential Monte Carlo sampling results, a fault occurred on line 0–1 at 903–907 h, with a duration of 5 h. The downstream load could not be supplied, and maximum island partitioning of the DN had to be carried out based on the output of DG devices and the remaining electricity information of the ES devices at each time point. Based on the calculation method detailed in Section 3.1, under the condition of no fault, the maximum output of the PV units and wind turbines and the remaining electricity of their configuration ES devices within that day are shown in Figure 7.

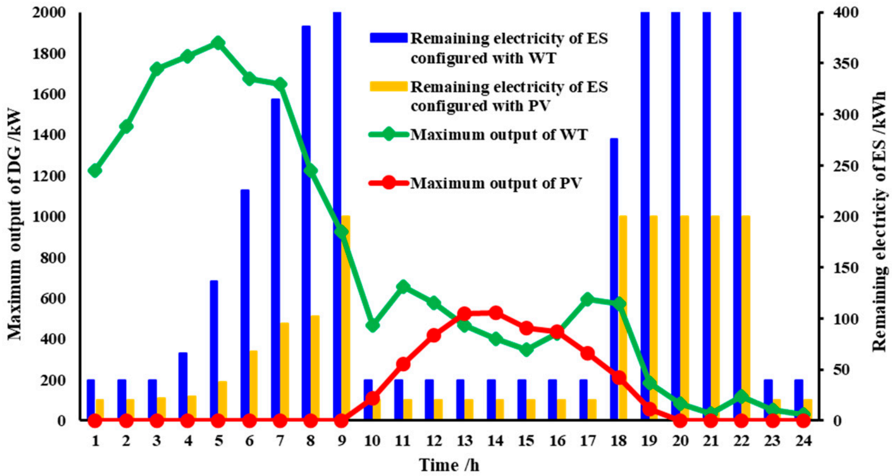

Figure 7. The DG active power and ES remaining electricity results.

We developed island partition schemes for the DN failure between 903 and 907 h. When generating the initial population using genetic algorithms, connectivity constraints need to be incorporated to ensure that all load nodes in the obtained islands meet the power supply rules. The number of genes and particles were both set to be 100, and the product of load power and priority weight was used as the fitness function. The convergence criterion was to optimize over 200 iterations. According to the introduction of Section 2, credible capacity searching is a one-dimensional search that requires continuous iteration until certain convergence criteria are met. The sequential Monte Carlo method was used, and system faults within a sampled year were generated through this method. To complete one power supply reliability estimation, about 10,000–50,000 sequential Monte Carlo simulations should be carried out. During the one-year Monte Carlo simulation, there were about 100 random failures. For each fault, respective island partition schemes were formulated to restore important loads in the DN. However, the sequential Monte Carlo calculation process took up a lot of time, while the island partition model should be solved in as little time as possible.

The island partitioning problem belongs to NP hard problems. Unless the solution space is traversed, the optimal solution cannot be mathematically guaranteed. A comparison of the island partition scheme and calculation time is provided in Table 2. In the genetic algorithm designed in this paper, the chromosomes do not indicate the state of each switch (i.e., open or closed), but, instead, the number of load nodes that are restored. According to the information of each chromosome, a potential recovery scheme can be specified under the premise of satisfying topological coherence, greatly avoiding the probability of infeasible solutions. After crossover and mutation operations, obvious infeasible solutions can be quickly eliminated according to the power and energy constraints.

Table 2. Island partition scheme based on genetic algorithm.

	Genetic Algorithm	Binary Particle Swarm Optimization	Differential Evolution Algorithm	Simulated Annealing Algorithm	Traversal Solving Algorithm
Calculation speed/s	24.59	421.10	65.19	710.02	uncontrollable
Island benefit	2.00×10^5	1.798×10^5	1.970×10^5	2.002×10^5	2.01×10^5

From the comparison, it can be seen that the method proposed in this paper was significantly faster than the binary particle swarm optimization [32], the differential evolution algorithm [33], the simulated annealing algorithm [34], and the traversal solving algorithm [35], of which the results obtained using the traversal solving algorithm could be regarded as the benchmark. Through comparison, it was found that the algorithm proposed in this paper can find a solution very close to the optimal solution in a relatively short period of time. The other algorithms took tens or even hundreds of seconds to solve the complex island partition model, while the proposed genetic algorithm provided the fastest solution speed while guaranteeing optimal results. The genetic algorithm can already meet engineering requirements. The range of the island partition scheme provided by the genetic algorithm is shown in Figure 8.

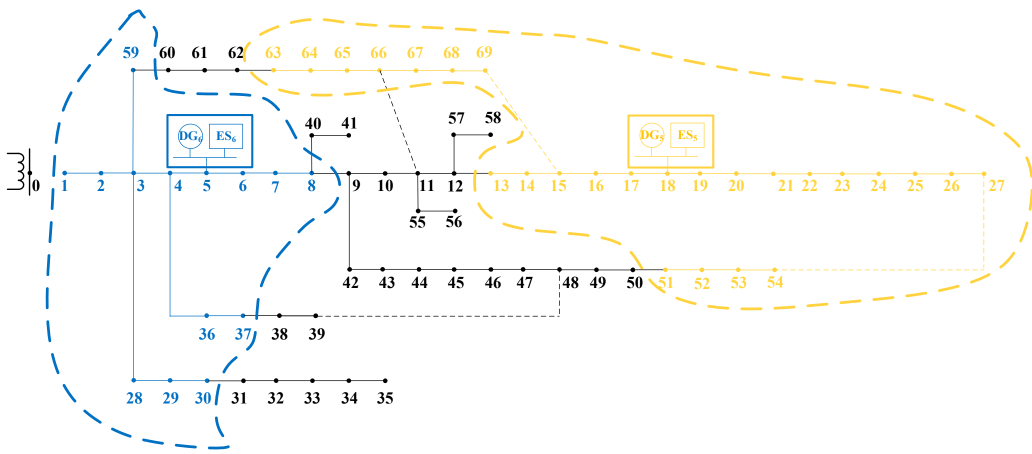

Figure 8. Island partition scheme based on the proposed genetic algorithm.

Under the island partition scheme developed using the method proposed in this paper, the remaining ES during the fault period is shown in Figure 9. The island partition scheme obtained when the ES devices are not connected to the power system and secondary power outage constraints are considered is shown in Figure 10. Due to the secondary power outage constraints, if the DG output is insufficient at certain times under the fault state, a large number of important loads cannot be restored. Comparing the presence and absence of ES devices in different scenarios, it was found that the integration of ES devices can provide emergency support for important loads under fault conditions.

4.3. Improved Effectiveness of Power Supply Capability Based on Credible Capacity

When selecting the EENS as a reliability indicator, the system's power shortage before the DG devices were connected was 2.241×10^5 kWh, which serves as the reliability benchmark. After the integration of 6 MW DG, the system's power supply reliability was improved, and the EENS decreased to 1.078×10^5 kWh. According to the binary method, continuous adjustment of the load demand level was made until the convergence criterion was met. The search process is shown in Figure 11. After six searches, it was found that when the load increased by 772.7 kW from the original level, the system's unserved electricity was 2.232×10^5 kWh, which met the convergence criterion under the principle of equal power supply reliability. The combination of 6 MW DG and 20%

ES increased the power supply capability of the DN by 772.7 kW, which is 12.88% of the installed capacity of DG.

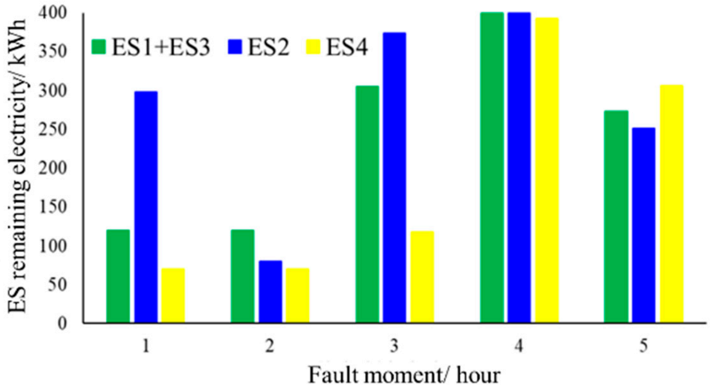

Figure 9. Fluctuation of ES remaining power.

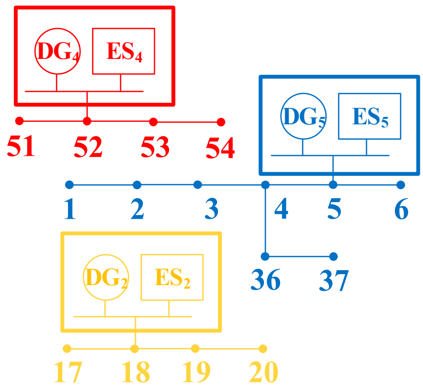

Figure 10. Island partition scheme without ES.

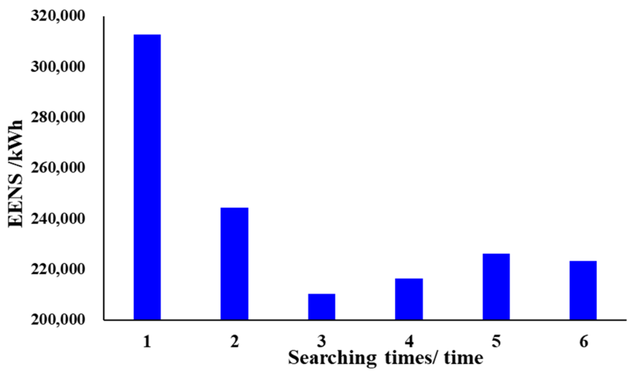

Figure 11. Credible capacity search results based on EENS index.

To reflect the impact of the selection of the reliability index on the reliability capacity evaluation results, we considered the EENS system power supply reliability rate [9] and system outage duration [30] as reliability indicators, in order to evaluate the reliability capacity of the DN. Taking the system power supply reliability rate and system outage duration as reliability indicators, the system's power supply reliability rate was 99.893% before the DG was connected, and the total outage duration of the system load was 241 h. After the 6 MW distributed power supply DG was connected, the power supply reliability of the system is 99.949%, and the total power outage duration of the system load was 112 h. The binary method was used to continuously search for the credible capacity value.

When the system load demand increased to 20.32% of the original level—that is, when the load increased by 772.7 kW—the power supply reliability rate of the system was 99.897%, meeting the equal reliability criterion based on the system's power supply reliability rate (as the reliability index). When the system load demand increased to 21.10% of the original level—that is, when the load increased by 802.3 kW—the total power outage duration of the system load was 244 h, meeting the equal reliability criterion based on the reliability index of the power system. According to the search results, it is not difficult to see that the difference in the credible capacity evaluation results was relatively small under the different reliability indicators, indicating that the credible capacity evaluation results were relatively stable.

The DG credible capacity evaluation results can inform the configuration of the proportion of ES devices and the installed DG capacity, which plays a guiding role in the operation and planning of power systems. Although the installed capacity of a single DG device is relatively small, the total credible capacity of thousands of DG devices will have an undeniable impact on the power system. The credible capacity of DG devices can be used in DNs for customer self-balancing and regional power balance analysis, and it has been applied in capacity market transactions abroad. For DN planning, the traditional approach of optimizing substations with load rates that meet $N-1$ conditions as constraints is changing. The credible capacity of DG devices can replace the traditional approach, and the investment in new substations can be reduced by more than 30% when the credible capacity index is considered in the planning stage. At present, the credible capacity index is regarded as the goal for optimizing the installed capacity of rooftop photovoltaic devices in certain intelligent communities. The effective coordination and optimization of multiple and massive controllable resources within power systems can be effectively achieved, in which it can be expected that the credible capacity index will play an important role.

5. Discussion

A method for evaluating the improvement of power supply capability in a distribution network (DN) based on credible capacity was proposed in the paper. The temporal fluctuation of the distributed generation (DG) output and load demand was considered during a fault period, and an island partition model considering the secondary power outage constraint was established. In reliability calculations, the expected energy not served (EENS) indicator was regarded as a reliability index, and the improvement of power supply capability can be obtained based on the DG–ES dichotomy. However, the island partition model with complex constraints cannot be solved easily. For convenience of solution, a modified genetic algorithm was proposed to solve the complex island partition model directly. Compared with common heuristic algorithms, such as the greedy algorithm, the proposed genetic algorithm obtained an island partition scheme with greater benefit at an appropriate speed, making it suitable for the optimal scheduling problem.

The improved PG&E 69-bus system was analyzed in the case study of this paper. Notably, the proposed method is universal for all radial distribution networks. According to the simulation results, the proposed method possesses a strong searching ability and excellent convergence performance. In the sensitivity analysis, considering the secondary power outage constraint during the fault period, configuring an appropriate proportion of energy storage (ES) can significantly improve the power supply capability of the DN. Moreover, the results suggested that the power supply capability improvement brought about by 6 MW DG can reach about 773 kW with a 20% configuration ratio of ES devices. As such, the capacity value of DG and ES devices cannot be ignored.

Furthermore, the IEEE 33-bus system is studied to enrich the results. The topology is shown in Figure 12. The installed capacities and integration nodes of DGs are as follows: node 7 with 1 MW PV, node 11 with 2 MW wind turbine, node 14 with 1 MW PV, node 29 with 2 MW wind turbine, and node 31 with 1 MW PV. The five interconnection switches are on the tie-lines of 7-20, 11-21, 8-14, 24-28, and 17-32, respectively. The failure rate is 0.2 times per year, and the repair rate is 1000 times per year. After the integration of 7 MW

DG, the EENS is decreased from 1.609×10^5 kWh to 7.689×10^4 kWh. We adjust the value of incremental load demand to meet the equal reliability criteria. The ΔL with a value of 1306.06 kW is locked. Therefore, the incremental power supply capability is 1.306 MW.

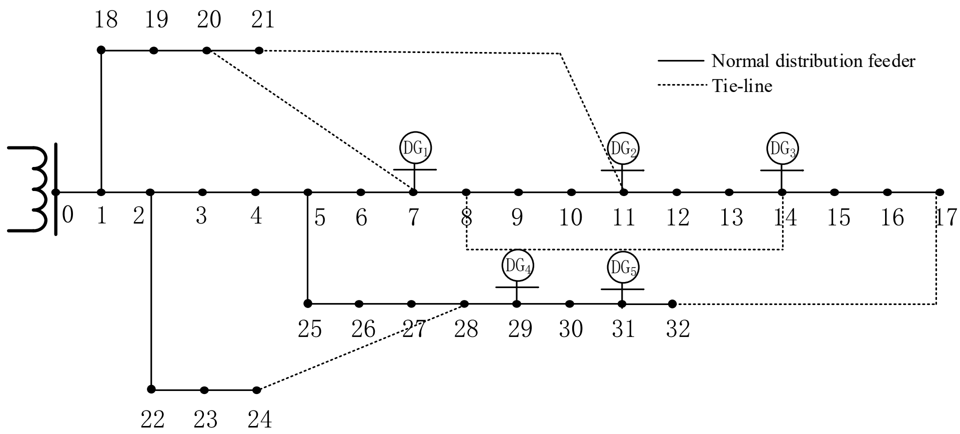

Figure 12. The topology of IEEE 33-bus system.

However, there still remain huge challenges regarding how to increase the calculation speed when using genetic algorithms. In the future research, the real-time monitoring data of micro-phasor measurement units on the operation status of a distribution network can be considered to improve the accuracy of load and distributed power output. In addition, the ES integration mode has an important effect on the power restoration ability under fault states. Our research team will continue to conduct in-depth research on the above challenges.

6. Conclusions

In this paper, we proposed a method for evaluation of the incremental power supply capability in a DN. The proposed method incorporates island partitioning as the core means of reliability evaluation in the credible capacity evaluation process, and the power supply capability is calculated incrementally with respect to credible capacity indicators. Through numerical analysis of the improved PG&E 69-bus system, we found the following:

(1) When considering the secondary power outage constraint during the fault period, configuring an appropriate proportion of ES devices can significantly improve the power supply capability during the fault period. Island partitioning is an important aspect of fault consequence analysis.

(2) With a 20% configuration ratio of ES devices, the power supply capability improvement brought about by 6 MW DG can reach about 773 kW, and the capacity value of DG and ES devices should be taken into consideration.

Author Contributions: Conceptualization, Y.H. and Z.H.; methodology, Y.H.; software, S.M.; validation, B.S., J.H. and J.C.; formal analysis, Z.H.; investigation, S.M.; resources, B.S.; data curation, J.C.; writing—original draft preparation, J.C.; writing—review and editing, B.S.; visualization, Y.H.; supervision, Z.H.; project administration, Z.H.; funding acquisition, Y.H. All authors have read and agreed to the published version of the manuscript.

Funding: This research was funded by "the State Grid scientific and technological projects of China, SGTYHT/21-JS-225 (SGTJDK00DWJS2200194)".

Data Availability Statement: Not applicable.

Conflicts of Interest: The authors declare no conflict of interest.

References

1. Sun, B.; Li, Y.; Zeng, Y.; Chen, J.; Shi, J. Optimization Planning Method of Distributed Generation Based on Steady-State Security Region of Distribution Network. *Energy Rep.* **2022**, *8*, 4209–4222. [CrossRef]
2. Sun, B.; Yu, Y.; Qin, C. Should China focus on the distributed development of wind and solar PV power generation? A comparative study. *Appl. Energy* **2017**, *185*, 421–439. [CrossRef]
3. Bagheri, A.; Monsef, H.; Lesani, H. Renewable power generation employed in an integrated dynamic DN expansion planning. *Electr. Power Syst. Res.* **2015**, *127*, 280–296. [CrossRef]
4. Zhao, J.; Zhang, M.; Yu, H.; Ji, H.; Song, G.; Li, P.; Wang, C.; Wu, J. An islanding partition method of active distribution networks based on chance-constrained programming. *Appl. Energy* **2019**, *242*, 78–91. [CrossRef]
5. Lin, W.; Zhu, J.; Yuan, Y.; Wu, H. Robust optimization for island partition of distribution system considering load forecasting error. *IEEE Access* **2019**, *7*, 64247–64255. [CrossRef]
6. Li, Z.; Khrebtova, T.; Zhao, N.; Zhang, Z.; Fu, Y. Bi-level service restoration strategy for active distribution system considering different types of energy supply sources. *IET Gener. Transm. Distrib.* **2020**, *14*, 4186–4194. [CrossRef]
7. Slota, G.M.; Root, C.; Devine, K.; Madduri, K.; Rajamanickam, S. Scalable, multi-constraint, complex-objective graph partitioning. *IEEE Trans. Parallel Distrib. Syst.* **2020**, *31*, 2789–2801. [CrossRef]
8. Ahmadipour, M.; Othman, M.M.; Salam, Z.; Alrifaey, M.; Ridha, H.M.; Veerasamy, V. Optimal load shedding scheme using grasshopper optimization algorithm for islanded power system with distributed energy resources. *Ain Shams Eng. J.* **2023**, *14*, 101835.
9. Chen, J.; Sun, B.; Li, Y.; Jing, R.; Zeng, Y.; Li, M. Credible capacity calculation method of DG based on equal power supply reliability criterion. *Renew. Energy* **2022**, *201*, 534–547. [CrossRef]
10. Popovic, Z.N.; Knezevic, S.D.; Brbaklic, B.S. A risk management procedure for island partitioning of automated radial distribution networks with distributed generators. *IEEE Trans. Power Syst.* **2020**, *35*, 3895–3905. [CrossRef]
11. Garver, L. Effective load carrying capability of generating units. *IEEE Trans. Power Appar. Syst.* **1966**, *PAS-85*, 910–919. [CrossRef]
12. Frew, B.; Cole, W.; Sun, Y.; Mai, T.T.; Richards, J. *8760-Based Method for Representing Variable Generation Capacity Value in Capacity Expansion Models*; National Renewable Energy Lab. (NREL): Golden, CO, USA, 2017.
13. D'Annunzio, C.; Santoso, S. Noniterative method to approximate the effective load carrying capability of a wind plant. *IEEE Trans. Energy Convers.* **2008**, *23*, 544–550. [CrossRef]
14. Dragoon, K.; Dvortsov, V. Z-method for power system resource adequacy applications. *IEEE Trans. Power Syst.* **2006**, *21*, 982–988. [CrossRef]
15. Zhang, N.; Kang, C.; Kirschen, D.; Xia, Q. Rigorous model for evaluating wind power capacity credit. *IET Renew. Power Gener.* **2013**, *7*, 504–513. [CrossRef]
16. Ding, M.; Xu, Z. Empirical model for capacity credit evaluation of utility-scale PV plant. *IEEE Trans. Sustain. Energy* **2016**, *8*, 94–103. [CrossRef]
17. Hou, Q.; Zhang, N.; Du, E.; Miao, M.; Peng, F.; Kang, C. Probabilistic duck curve in high PV penetration power system: Concept, modeling, and empirical analysis in China. *Appl. Energy* **2019**, *242*, 205–215. [CrossRef]
18. Rathore, A.; Patidar, N.P. Reliability assessment using probabilistic modelling of pumped storage hydro plant with PV-Wind based standalone microgrid. *Int. J. Electr. Power Energy Syst.* **2019**, *106*, 17–32. [CrossRef]
19. Tawfeek, T.S.; Ahmed, A.H.; Hasan, S. Analytical and particle swarm optimization algorithms for optimal allocation of four different distributed generation types in radial distribution networks. *Energy Procedia* **2018**, *153*, 86–94. [CrossRef]
20. Wang, S.; Zheng, N.; Bothwell, C.D.; Xu, Q.; Kasina, S.; Hobbs, B.F. Crediting Variable Renewable Energy and Energy Storage in Capacity Markets: Effects of Unit Commitment and Storage Operation. *IEEE Trans. Power Syst.* **2022**, *37*, 617–628. [CrossRef]
21. Paik, C.; Chung, Y.; Kim, Y. ELCC-based capacity credit estimation accounting for uncertainties in capacity factors and its application to solar power in Korea. *Renew. Energy* **2021**, *164*, 833–841. [CrossRef]
22. Chen, F.; Li, F.; Feng, W.; Wei, Z.; Cui, H.; Liu, H. Reliability assessment method of composite power system with wind farms and its application in capacity credit evaluation of wind farms. *Electr. Power Syst. Res.* **2019**, *166*, 73–82. [CrossRef]
23. IEEE Standard 1547.4–2011*IEEE Guide for Design, Operation, and Integration of Distributed Resource Island Systems with Electric Power Systems*; IEEE Standards Association: Piscataway, NJ, USA, 2011.
24. Ge, L.; Liu, H.; Yan, J.; Zhu, X.; Zhang, S.; Li, Y. Optimal Integrated Energy System Planning with DG Uncertainty Affine Model and Carbon Emissions Charges. *IEEE Trans. Sustain. Energy* **2022**, *13*, 905–918. [CrossRef]
25. He, X.; Geng, H.; Mu, G. Modeling of wind turbine generators for power system stability studies: A review. *Renew. Sustain. Energy Rev.* **2021**, *143*, 110865.
26. Sukriti, T.; Ashwani, K. Hybrid Taguchi-based Technique for Micro-phasor Measurement Units Placement in the Grid-connected Distribution System. *IETE J. Res.* **2021**, 1–13. [CrossRef]
27. Xu, K.; Yan, J.; Zhang, H.; Han, S.; Liu, Y. Quantile based probabilistic wind turbine power curve model. *Appl. Energy* **2021**, *296*, 116913. [CrossRef]
28. Zheng, B.; Wei, W.; Chen, Y.; Han, S.; Liu, Y. A peer-to-peer energy trading market embedded with residential shared energy storage units. *Appl. Energy* **2022**, *308*, 118400. [CrossRef]
29. Chen, X.; Qiu, J.; Reedman, L.; Dong, Z.Y. A statistical risk assessment framework for distribution network resilience. *IEEE Trans. Power Syst.* **2019**, *34*, 4773–4783. [CrossRef]

30. Moghaddam, M.; Kalam, A.; Nowdeh, S.; Ahmadi, A.; Babanezhad, M.; Saha, S. Optimal sizing and energy management of stand-alone hybrid PV/wind system based on hydrogen storage considering LOEE and LOLE reliability indices using flower pollination algorithm. *Renew. Energy* **2019**, *135*, 1412–1434. [CrossRef]
31. Yan, F.; Chen, X.; Tang, W.; Yan, R.; Wu, H. Reliability and Power Supply Capability Evaluation of Active Distribution Networks with Four-terminal Soft Open Points. *IET Smart Grid* **2020**, *3*, 657–666. [CrossRef]
32. Monteiro, R.; Bonaldo, J.; Silva, R.; Bretas, A.S. Electric distribution network reconfiguration optimized for PV distributed generation and energy storage. *Electr. Power Syst. Res.* **2020**, *184*, 106319. [CrossRef]
33. Qiao, B.; Liu, J. Multi-objective dynamic economic emission dispatch based on electric vehicles and wind power integrated system using differential evolution algorithm. *Renew. Energy* **2020**, *154*, 316–336. [CrossRef]
34. Tabak, A.; İlhan, İ. An effective method based on simulated annealing for automatic generation control of power systems. *Appl. Soft Comput.* **2022**, *126*, 109277. [CrossRef]
35. Wang, C.; Ge, P.; Sun, L.; Wang, F. Research on user-side flexible load scheduling method based on greedy algorithm. *Energy Rep.* **2022**, *8*, 192–201. [CrossRef]